Electron transmission through an ac biased quantum point contact

Almas F. Sadreev[1,2,*] and Kirill Davlet-Kildeev[1]
[1]*Institute of Physics, Academy of Sciences, 660036 Krasnoyarsk, Russia*
[2]*Department of Physics and Measurement Technology, Linköping University, S-581 83 Linköping, Sweden*
(Received 10 October 2006; revised manuscript received 23 February 2007; published 7 June 2007)

We consider a transmission through the potential relief created by a split gate constriction (quantum point contact). Simultaneously, dc and ac voltages $V_{up}(t)=V_0+V_1\cos\omega t$ and $V_{dw}(t)=V_0+V_1\cos(\omega t+\theta)$ are applied to the gates. We show numerically that the in-phase ac voltages ($\theta=0$) smear the conductance steps of the stationary conductance, while the antiphase ac voltages ($\theta=\pi$) only shift the conductance steps. Moreover, computation of currents in probing wires connected cross to the time-periodic quantum point contact reveals a net current for $\theta\neq 0,\pi$. This implies that the Schrödinger equation described by the electron transport under the effect of the time-periodic long electrodes is equivalent to the transmission in the crossed effective magnetic and electric fields, where the in-plane magnetic field $\mathbf{b}\sim\theta$ is directed along the transport axis and the electric field $\mathbf{e}\sim\omega$ is directed perpendicular to the plane of electron transport. Then the vector $\mathbf{e}\times\mathbf{b}$ gives rise to the galvanomagnetic current directed cross to the electron transport.

DOI: 10.1103/PhysRevB.75.235309 PACS number(s): 73.63.−b, 72.10.−d, 72.30.+q

I. INTRODUCTION

Recent decades have seen rapid development in experiment and theory on "quantum devices," structures whose dimensions are comparable with the wavelength of electrons within them.[1] Ballistic electronic devices are typically based on a two-dimensional electron gas (2DEG) in a III-V heterostructure where scattering is small because of the separation between the donors and electrons. The electrons are then guided by electrostatic fields produced by patterned gates on the surface of the structure to produce long wires (equivalent to electromagnetic waveguides) as well as short wires or quantum point contacts.[2–4]

It is known that the conductance of a one-dimensional ballistic wire is quantized in units of $2e^2/h$. This was discovered experimentally[2–4] in split gate induced constrictions in high-mobility 2DEGs. Both experimental[5] and theoretical results[6–10] have shown that the accuracy of the observed quantization is sensitive to the detailed shape of a confining potential and the presence of impurities. Essential advantages of this system are its reduced dimensionality and lower electron-gas density, with correspondingly large Fermi wavelength, which can be varied locally by means of gate electrodes. Point contacts of variable width of the order of the Fermi wavelength have been defined by applying a negative voltage to a split gate on top of the heterostructure. A view of the split gate is presented in Fig. 1(a), which consists of wide straight electron waveguide with the split gate above the waveguide. The confining potential results in the shape of a quantum point contact (QPC) as shown in Fig. 1(b).

In the present work, we consider the transmission through the split gate biased by the dc and ac voltages

$$V_{up}(t) = V_0 + V_1\cos(\omega t), \quad V_{dw}(t) = V_0 + V_2\cos(\omega t + \theta), \tag{1}$$

both applied to the upper and lower gates, respectively. If the waveguides were closed, the device could serve as an electron pump[11,12] that generates dc between two probe electrodes that are kept at the same bias. In recent years, electron pumps consisting of small semiconductor quantum dots have received considerable experimental[13,14] and theoretical attention.[15–22] Then one can expect that a similar mechanism could give rise to the output currents in two probing wires

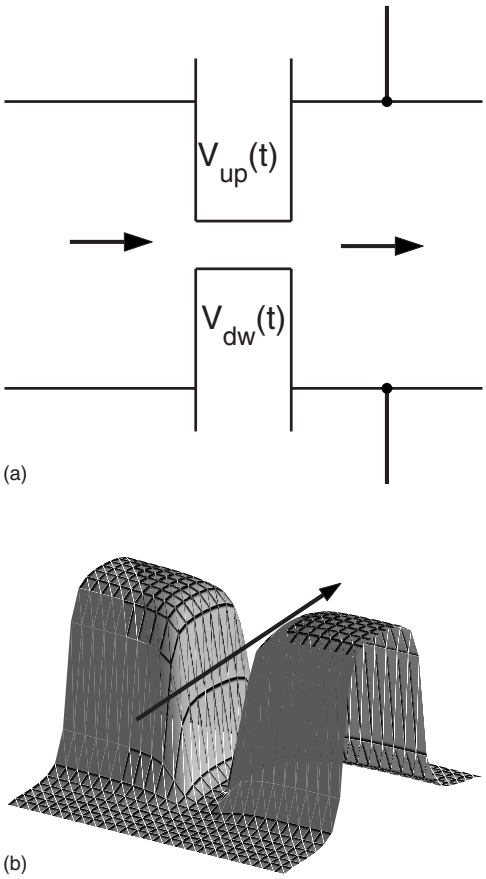

FIG. 1. (a) A wide straight waveguide with implied split gate on top of the heterostructure. Voltages (1) are applied to the gates. (b) The potential relief (2) created by the split gate with applied dc voltage V_0 for $V_1=0$. The bold arrow shows electron flow through the potential.

shown in Fig. 1(a) not being equal to each other for electron flow in an open waveguide through the QPC. Hence we expect the pumped Hall-like effect because of the phase difference in ac voltages. Moreover, we justify this effect by equivalence of the system to the electron transmission in crossed electric and magnetic fields. The aim of the present paper is to demonstrate the Hall-like effect for the transmission through the ac biased QPC provided that the phases of the ac voltages applied to the gates differ. We calculate the conductance of QPC as dependent on the Fermi energy of incident electrons E, the frequency of the ac voltages, and the phase difference θ.

II. TIME-PERIODIC POTENTIAL

The solution for potential profiles created by patterned polygon gates is given by Davies *et al.*[23] For the form of gates shown in Fig. 1(a) (split gate wire), the solution can be presented as

$$V(x,y,t) = \sum_{\alpha=up,low} V_\alpha(t) v_\alpha(x,y),$$

$$v_{up}(x,y) = \frac{1}{2\pi}\arctan\frac{d+x}{h} + \frac{1}{2\pi}\arctan\frac{d-x}{h} - g(a+y,d+x) - g(a+y,d-x),$$

$$v_{low}(x,y) = \frac{1}{2\pi}\arctan\frac{d+x}{h} + \frac{1}{2\pi}\arctan\frac{d-x}{h} - g(a-y,d+x) - g(a-y,d-x), \quad (2)$$

where

$$g(u,v) = \frac{1}{2\pi}\arctan\frac{uv}{hR}, \quad R = \sqrt{x^2+y^2+h^2},$$

a is half of the gap of the split gate, d is half of the width of gates, h is the depth of 2DEG, and α counts the upper and lower gates shown in Fig. 1(a).

The stationary potential for $V_1=0$ and $V_2=0$ is shown in Fig. 1(b). Profiles of the confining potential (2) for the different phases and times are shown in Fig. 2. One can see from Fig. 2(a) that for $\theta=0$, the in-phase ac voltages modulate the width of QPC for the fixed Fermi energy. If the phases differ by π, the antiphase ac voltages give rise to effective harmonic vibration of QPC cross to the transport axis as shown in Fig. 2(b). A similar problem was considered by Tang and Chu,[24] who studied the quantum transport in a narrow constriction which is acted upon by an external time-dependent electric field. However, the essential difference is that, in our case, two gates responsible for the narrow constriction are time dependent. Moreover, we allow the ac voltages of the gates to have different phases.

III. GENERAL EQUATIONS

The methods of numerical calculation of the conductance through one-dimensional time-periodic potentials are well developed.[25–29] The development of the method for two-dimensional structures is straightforward. We assume that electrons are incident to the two-dimensional waveguide with the width L. Then the wave functions of electrons in the pth subband incident from the left are

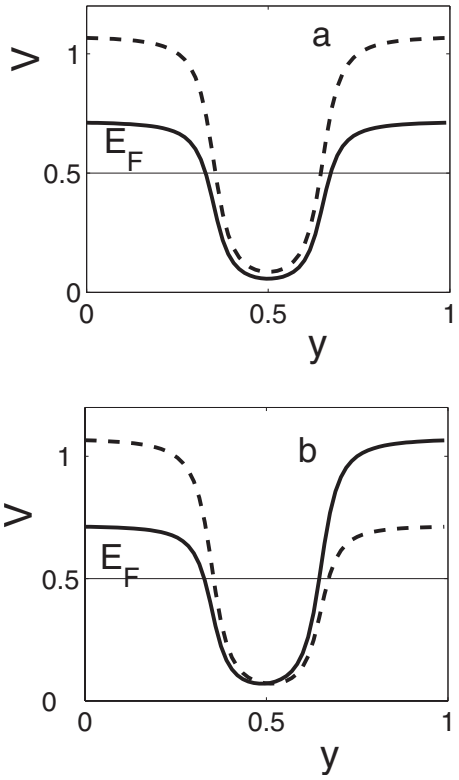

FIG. 2. Profiles of the time-periodic QPC potential (2) cross to the transport axis for $\omega t=\pi/2$ (solid lines) and $\omega t=3\pi/2$ (dashed lines). (a) $\theta=0$ and (b) $\theta=\pi$.

$$\psi_p(x,y,t) = \frac{1}{\sqrt{2\pi k_p}}\phi_p(y)e^{ik_p x - iEt}, \quad (3)$$

where

$$\phi_p(y) = \sqrt{2}\sin(\pi p y), \quad p = 1,2,3,\ldots, \quad (4)$$

$$E = k_p^2 + \pi^2 p^2. \quad (5)$$

The energy E is measured in terms $E_0=\hbar^2/2m^*L^2$, and the Cartesian coordinates x,y are measured in terms of the width L. For the transmission through QPC, the electron undergoes a transition to the different subbands p'. Moreover, because of the time-periodic modulation of the QPC potential, the incident electron acquires the quasienergies $E+n\omega$, $n=0,\pm1,\pm2,\ldots$. In order to formulate the problem in terms of the transmission and reflection amplitudes, we assume that the potential of QPC gates can be neglected at long distance from QPC. In practice, this distance exceeds the depth h of the 2DEG. Therefore we can split the whole space into three parts, the left incoming lead, the right outgoing lead, and the region of the time-periodic QPC. Then the solution of the time-dependent Schrödinger equation in the leads can be written analytically:

$$\psi_p(x,y,t) = \begin{cases} e^{ik_p x}\varphi_p(y)e^{-iEt} + \sum_{p'm} r_{pp'm}e^{-ik_{p'm}x}\varphi_{p'}(y)e^{-i(E+m\omega)t} & \text{left} \\ \sum_{p'm} t_{pp'm}e^{ik_{p'm}x}\varphi_{p'}(y)e^{-i(E+m\omega)t} & \text{right}, \end{cases} \tag{6}$$

where

$$E + m\omega = k_{pm}^2 + \pi^2 p^2,$$

$$\varphi_p(y) = \sqrt{2}\sin \pi p y. \tag{7}$$

In the scattering region with the time-periodic potential (2), we present the wave function as

$$\psi(x,y,t) = \sum_m \psi_m(x,y)e^{-i(E+m\omega)t}.$$

Then the Schrödinger equation takes the following form:

$$(E+m\omega)\psi_m(x,y) = -\nabla^2\psi_m(x,y) + V_0\sum_\alpha v_\alpha(x,y)\psi_m(x,y) + \frac{1}{2}\sum_\alpha V_\alpha v_\alpha(x,y)[\psi_{m+1}(x,y)e^{i\theta_\alpha} + \psi_{m-1}(x,y)e^{-i\theta_\alpha}], \tag{8}$$

where the index α enumerates the gates.

We approximate this equation by the finite-difference one introducing the grid $x=a_0 l$, $y=a_0 j$, where $l=0,1,2,\ldots,N_x+1$ and $j=1,2,3,\ldots,N_y$, $L_x=a_0N_x$, and $d=a_0N_y=1$. L_x is the length of the scattering region:

$$a_0^2(E+m\omega)\psi_m(l,j) = \psi_m(l+1,j) + \psi_m(l-1,j) + \psi_m(l,j+1) + \psi_m(l,j-1) - 4\psi_m(l,j) + a_0^2V_0\sum_\alpha v_\alpha(l,j)\psi_m(l,j) + \frac{1}{2}\sum_\alpha a_0^2V_\alpha v_\alpha(l,j)$$
$$\times[\psi_{m+1}(l,j)e^{i\theta_\alpha} + \psi_{m-1}(l,j)e^{-i\theta_\alpha}]. \tag{9}$$

In order to obtain the closed system of equations, we have to substitute into this equation the wave functions of the leads (6) for the slices $l=0$ and $l=N_x+1$, respectively,

$$\psi_p(l,j,t) = \begin{cases} e^{ik_p a_0 l}\varphi_p(j)e^{-iEt} + \sum_{p'm} r_{pp'm}e^{-ik_{p'm}a_0 l}\varphi_{p'}(j)e^{-i(E+m\omega)t} & \text{left} \\ \sum_{p'm} t_{pp'm}e^{ik_{p'm}a_0 l}\varphi_{p'}(j)e^{-i(E+m\omega)t} & \text{right}, \end{cases} \tag{10}$$

where Eqs. (7) are modified the finite-difference approximation as follows:

$$a_0^2(E+m\omega) = 4 - 2\cos k_{pm}a_0 - 2\cos\frac{\pi p a_0}{N_y+1},$$

$$\varphi_p(j) = \sqrt{\frac{2}{N_y+1}}\sin\frac{\pi p j}{N_y+1}. \tag{11}$$

Finally, substituting Eq. (10) into Eq. (9) for the slices $l=0$ and $l=N_x+1$, respectively, we obtain the inhomogeneous system of linear algebraic equations, which can be written in the following matrix form:

$$\tilde{H}\vec{\Psi} = \vec{g}, \tag{12}$$

where $\tilde{H}$ is the matrix of rank $N=(N_x+2)N_y(2M+1)$, $\vec{\Psi}$ is the vector of the same dimension N of the $N_y(2M+1)$ amplitudes of the reflection $r_{pp'm}$, $m=-M,-M+1,\ldots,M-1,M$, of the same number of the amplitudes of the transmission $t_{pp'm}$, and the $N_xN_y(2M+1)$ number of the amplitudes $\psi_m l,j$ specified the wave function in the scattering region.

We define the conductance G as a ratio of output current to the input one.[30,31] In the tight-binding approximation, the current-density component along the incident direction can be evaluated as[32]

$$j_x(l,j) = j_0\,\overline{\mathrm{Im}[\psi^*(l,j)\psi(l+1,j)]}, \quad j_0 = \frac{e\hbar}{2m^*d}, \tag{13}$$

which is transformed into the well-known quantum-mechanical expression for the current density in the continual limit $a_0\to 0$. Here, $\overline{\cdots}=\frac{1}{T}\int_0^T dt\ldots$ means an average of the period of oscillations. After substitution of Eq. (10) into Eq. (13), integration over the lead section, and averaging over the period of oscillations, we obtain the input current $J_{in}=j_0\sin(k_{p0}a_0)$ and the output current $J_{out}=j_0\Sigma_{p'm}|t_{pp'm}|^2\sin(k_{p'm}a_0)$. Therefore the conductance equals

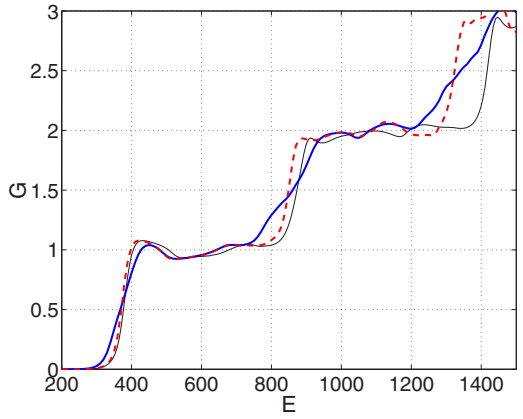

FIG. 3. (Color online) Conductance G of QPC in terms of $2e^2/h$ versus energy of incident electrons E in terms of $\hbar^2/2m^*L^2$. QPC is formed by two split gates shown in Fig. 1(a) biased by the voltages given in Eq. (1) with $V_0=2000$, $V_1=400$, and $\omega=0.2$. Thin solid line corresponds to the stationary transmission with $V_1=0$, thick solid line corresponds to $\theta=0$ (in-phase modulation of QPC), and dashed line corresponds to $\theta=\pi$ (antiphase modulation of QPC). The parameters of QPC constriction are the following: half of the gap of QPC, $a=0.1$; half of the width of gates, $d=0.2$; and the depth of 2DEG, $h=0.02$, in terms of the waveguide's width.

$$G = \sum_{p'm} \frac{\sin k_{p'm}a_0}{\sin k_{p0}a_0}\overline{|t_{pp'm}|^2}, \tag{14}$$

which reduces to the standard expression for the conductance in the continual approximation.[29,30]

IV. TIME-PERIODIC QPC

First, we consider the conductance of the time-periodic QPC without probing wires. The results of computation for the conductance versus the Fermi energy are shown in Fig. 3.

For the stationary case, one can see that the conductance is approximately quantized by the value $2e^2/h$ with oscillations, because of the quantum interference due to the finite length of QPC as is well known.[6–10] Although the case of the antiphase ac voltages does not change the width of QPC compared to the stationary case as shown in Fig. 2(b), one can see from Fig. 3 that the conductance steps shift to lower energies. The in-phase ac voltages give rise to smearing of the conductance steps as shown in Fig. 3 by the thick solid line. This effect is a result of the fact that the characteristic times of the electron transmission through QPC of order $1/\sqrt{E}\sim 10^{-1}-10^{-2}$ are much shorter than the period of oscillation of the QPC width. Therefore, for the transmission through the in-phase ac biased QPC, electrons effect an adiabatic slow variation of the QPC width that resulted in smearing of the conductance steps. Indeed, computation of the conductance for ultrafast in-phase oscillations $\omega \gg \sqrt{E}$ shows that the conductance steps are restored and coincided with the case of the antiphase ac voltages, while variation of the frequency of the ac voltages up to $\omega \leqslant \sqrt{E}$ has no effect in comparison to $\omega=0.2$ as shown in Fig. 3.

V. HALL-LIKE EFFECT

Consider at first the model case of infinite thin wires directed along the x axis and located at $y=y_\alpha$, with applied voltages $V_\alpha=V_0+V_1\cos(\omega t+\theta_\alpha)$. Then Eq. (8) in tight-binding approximation along the y axis can be written as follows:

$$(E+m\omega+k_x^2)\psi_{m,\alpha} = \gamma(\psi_{m,\alpha+1}+\psi_{m,\alpha-1}) + \frac{1}{2}V_1[\psi_{m+1,\alpha}e^{i\theta_\alpha} + \psi_{m-1,\alpha}e^{-i\theta_\alpha}], \tag{15}$$

where γ is the tunneling amplitude between the neighboring wires. This equation describes effectively a tight-binding chain enumerated by sites α with the time-periodic potentials $V_\alpha(t)=V_1\cos(\omega t+\theta_\alpha)$ applied at the sites of the chain. Such a chain wire directed along the y axis was considered in Ref. 21. An existence of pumped current along the y axis was shown. Therefore for the electron transport along the x axis, one can expect pumped current along the y axis; in other words, the Hall-like effect. Hence, one can expect a similar net current in the y axis even for two gates formed by QPC provided that they are biased by the ac voltages with different phases.

Equation (15) allows us to interpret the Hall-like effect as related to a galvanomagneticlike one in crossed effective magnetic and electric fields. Let us take the phase of the αth wire as $\theta_\alpha=\theta_0\alpha$. Consider an effective constant magnetic field $b=\theta_0$ directed along the x axis. The corresponding vector potential can be chosen as $\mathbf{a}=(0,0,by)$, where we introduced a new auxiliary axis (z axis). This axis is given by sites m with the hopping matrix elements $V_1/2$ in Eq. (15) and similar to Eq. (9). Then the Peierls phase factor[33,34] $\exp(ib\alpha)=\exp(i\theta_0\alpha)$ is to be substituted along the z axis at each $\psi_{m+1,\alpha}$. Correspondingly, at each $\psi_{m-1,\alpha}$, the complex conjugated Peierls phase factor is to be substituted, i.e., just as shown in the last term of Eq. (15). Note that this analog of the phase difference θ_0 to the effective magnetic field is applicable for small θ_0.[34] Next, Eq. (15) shows that along the z axis the effective constant electric field ω is applied. Therefore, Eq. (15) effectively describes the three-dimensional motion of an electron homogeneous along the x axis, discrete along the y axis with the hopping matrix elements γ, and discrete along the z axis with hopping matrix elements $V_1/2$. Moreover, the electron moves in the crossed effective electric field $e=\omega$ directed along the z axis and the effective magnetic field $b=\theta_0$ directed along the x axis. Then the vector $\mathbf{e}\times\mathbf{b}$ directed along the y axis violates the symmetry relative to $y\to -y$ and gives rise to the galvanomagnetic current[35]

$$j_y = \sigma_{yxz}eb \sim \omega\theta_0 \tag{16}$$

for small ω and θ_0. Numerical calculations completely confirm this consideration even for two wires ($\alpha=1,2$) provided that the ac voltages applied to them have a phase difference. As Fig. 4 shows, the effect is odd relative to the frequency of oscillations of QPC.

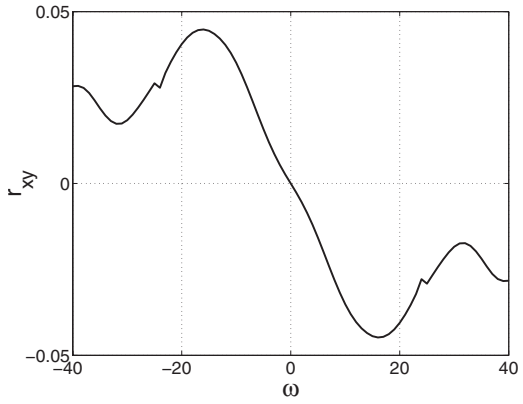

FIG. 4. The magnetoresistance given by formula (17) versus frequency of oscillations for $\theta=\pi/2$, energy $E=1500$, dc voltage $V_0=2000$, and ac voltage $V_1=400$. The parameters of the split gate are the same as in Fig. 3.

Following Peeters[36] and Akera and Ando,[37] we take the waveguide connected to electron reservoirs with chemical potentials μ_L and μ_R, and $\mu_L-\mu_R$ is positive infinitesimal. Moreover, we take that the waveguide is connected to the upper and lower Hall contacts, as shown in Fig. 1(a). The probes were modeled by the one-dimensional wires connected to the waveguide via hopping matrix element in tight-binding approach to simulate the weak-link model.[36] Following Ref. 37, we introduce the magnetoresistance as

$$R_{xy}=\frac{h}{2e^2}r_{xy},\quad r_{xy}=\frac{T_{up}-T_{dw}}{T_{up}+T_{dw}},\tag{17}$$

where T_α, $\alpha=$up and dw, are the transmission probabilities in the upper and lower probing wires, respectively. In order to find the transmission probabilities, we write the output states in the probing wires as follows:

$$\psi_\alpha(y,t)=\sum_m t_{\alpha,m}\exp(\pm ik_{wm}y-iEt-im\omega t),\tag{18}$$

where $E+m\omega=k_{wm}^2+\Delta$. The auxiliary parameter Δ is introduced in order that the wave numbers of the probing wires k_{wm} were real for the incident energy E. In other words, the role of Δ is to compensate the difference between propagation bands of the wide waveguide and the narrow probing wire. Then, from Eq. (18), we obtain the transmission probabilities

$$T_\alpha=\sum_m \overline{|t_{\alpha,m}|^2},\quad \alpha=\text{up and dw}.\tag{19}$$

Results of numerical computation for the Hall resistance are shown in Figs. 5 and 6. Numerically, we have to restrict the number of the quasienergies labeled by the integer $m=0,\pm1,\pm2,\ldots$. Empirically, we chose $M\geqslant|m|$ for a given amplitude of the ac voltage such that $M\to M+1$ gives no visible modification of the results. In practice, we chose $M=3,4$.

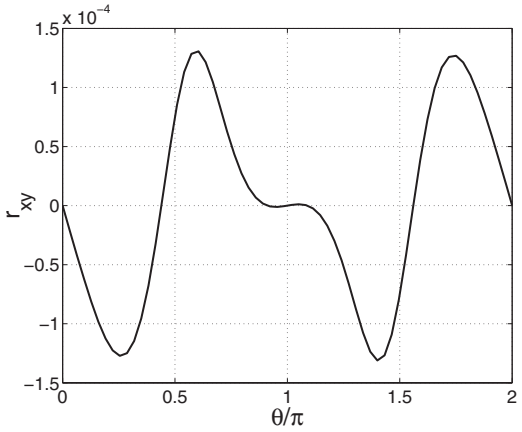

FIG. 5. The magnetoresistance versus θ for energy $E=1500$, dc voltage $V_0=2000$, ac voltage $V_1=400$, and $\omega=0.1$. The parameters of the split gate are the same as in Fig. 3.

VI. CONCLUDING REMARKS

In conclusion, we present dimensional estimations of the results. Taking the typical width of the electron waveguide as 1 μm, we have the characteristic energy $E_0\approx5\times10^{-2}$ meV. For the dc voltage of the split gate of order 1 V, we have $V_0\sim10^4$. The dimensionless frequency equals $\omega=\hbar\Omega/E_0$. For the ac frequency $\Omega=10^7$ Hz,[13] we obtain $\omega\approx10^{-4}$. Correspondingly, for $\Omega=1$ GHz, we have $\omega=0.01$, while the characteristic traveling time through QPC is of order $1/\sqrt{E}\gg1$. Therefore, for the micron devices, the ac voltage can be considered as an adiabatic process. However, as Fig. 4 shows, the linear behavior of the magnetoresistance r_{xy} is preserved up to $|\omega|\lesssim5$. Finally, for the ac gate voltage of order 100 mV, we obtain the amplitude of the time-periodic perturbation $V_1\sim10^4$.

Our computations of the transmission through the ac biased QPC show two interesting results. The first is a smearing of the conductance steps for $\theta=0$, which is caused by the oscillation of the width of the QPC as shown in Fig. 3. The second result is that the phase difference $\theta\neq0,\pi$ of the ac gate voltages results in the Hall-like

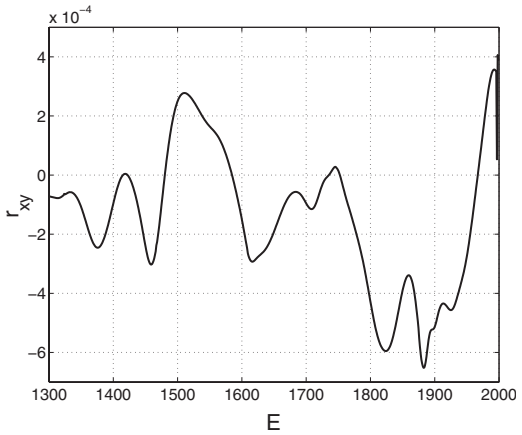

FIG. 6. The Hall resistance versus the Fermi energy E for the dc voltage $V_0=2000$, the ac potential $V_1=400$, $\omega=0.2$, and the phase difference $\theta=\pi/2$.

effect measured by probing wires connected as shown in Fig. 1(a). The effect was interpreted such that the Schrödinger equation described by the electron transport under the effect of the time-periodic long electrodes is equivalent to the discrete three-dimensional electron motion in the crossed effective electric and magnetic fields, where the electric field $\mathbf{e} \sim \omega$ is directed along the z axis and the magnetic field $\mathbf{b} \sim \theta$ is directed along the transport axis. Then the vector $\mathbf{e} \times \mathbf{b}$ gives rise to the galvanomagnetic current directed along the y axis cross to the electron transport.

ACKNOWLEDGMENTS

A.F.S. thanks K.-F. Berggren for discussions. This work has been supported by RFBR Grant No. 07-02-00304.

*Email addresses: almsa@ifm.liu.se and almas@tnp.krasn.ru

[1] J. H. Davies and A. R. Long, *Physics of Nanostructures* (Institute of Physics, Bristol, 1992); (Institute of Physics, Bristol, 1988), p. 848.
[2] K.-F. Berggren, T. J. Thornton, D. J. Newson, and M. Pepper, Phys. Rev. Lett. **57**, 1769 (1986).
[3] B. J. van Wees, H. van Houten, C. W. J. Beenakker, J. G. Williamson, L. P. Kouwenhouen, D. van der Marel, and C. T. Foxon, Phys. Rev. Lett. **60**, 848 (1988).
[4] D. A. Wharam *et al.*, J. Phys. C **21**, L209 (1988).
[5] J. G. Williamson, C. E. Timmering, C. J. P. M. Harmans, J. J. Harris, and C. T. Foxon, Phys. Rev. B **42**, 7675 (1990).
[6] A. Szafer and A. D. Stone, Phys. Rev. Lett. **62**, 300 (1989).
[7] E. G. Haanappel and D. van der Marel, Phys. Rev. B **39**, 5484 (1989).
[8] D. van der Marel and E. G. Haanappel, Phys. Rev. B **39**, 7811 (1989).
[9] E. Tekman and S. Ciraci, Phys. Rev. B **39**, 8772 (1989).
[10] S. He and S. Das Sarma, Phys. Rev. B **40**, 3379 (1989).
[11] D. J. Thouless, Phys. Rev. B **27**, 6083 (1983).
[12] M. Büttiker, H. Thomas, and A. Prêtre, Z. Phys. B: Condens. Matter **94**, 133 (1994).
[13] M. Switkes, C. M. Marcus, K. Campman, and A. C. Gossard, Science **283**, 1905 (1999).
[14] L. DiCarlo, C. M. Marcus, and J. S. Harris, Phys. Rev. Lett. **91**, 246804 (2003).
[15] P. W. Brouwer, Phys. Rev. B **58**, R10135 (1998).
[16] B. L. Altshuler and L. I. Glazman, Science **283**, 1864 (1999).
[17] Y. Wei, J. Wang, and H. Guo, Phys. Rev. B **62**, 9947 (2000).
[18] O. Entin-Wohlman, A. Aharony, and Y. Levinson, Phys. Rev. B **65**, 195411 (2002).
[19] M. Blaauboer, Phys. Rev. B **68**, 205316 (2003).
[20] M. Moskalets and M. Buttiker, Phys. Rev. B **66**, 205320 (2002); **69**, 205316 (2004).
[21] E. Faizabadi and F. Ebrahimi, J. Phys.: Condens. Matter **16**, 1789 (2004).
[22] L. Arachea, Phys. Rev. B **72**, 125349 (2005).
[23] J. H. Davies, I. A. Larkin, and E. V. Sukhorukov, J. Appl. Phys. **77**, 4504 (1995).
[24] C. S. Tang and C. S. Chu, arXiv:cond-mat/0603480 (unpublished); arXiv:cond-mat/0603543 (unpublished).
[25] M. Buttiker and R. Landauer, Phys. Rev. Lett. **49**, 1739 (1982).
[26] D. L. Haavig and R. Reifenberger, Phys. Rev. B **26**, 6408 (1982).
[27] M. Wagner, Phys. Rev. B **57**, 11899 (1998).
[28] C. P. del Valle, R. Lefebvre, and O. Atabek, Phys. Rev. A **59**, 3701 (1999).
[29] W. Li and L. E. Reichl, Phys. Rev. B **60**, 15732 (1999).
[30] M. Buttiker, Phys. Rev. B **38**, 9375 (1988).
[31] H. Kasai, K. Mitsutake, and A. Okiji, J. Phys. Soc. Jpn. **60**, 1679 (1991).
[32] K. N. Pichugin and A. F. Sadreev, Phys. Rev. B **56**, 9662 (1997).
[33] R. E. Peierls, Z. Phys. **80**, 763 (1933).
[34] G. Edwards, A. Grincwajg, and D. K. Ferry, Surf. Sci. **361/362**, 714 (1996).
[35] B. Abeles and S. Meiboom, Phys. Rev. **95**, 31 (1954).
[36] F. M. Peeters, Phys. Rev. Lett. **61**, 589 (1988).
[37] H. Akera and T. Ando, Phys. Rev. B **39**, 5508 (1989); **41**, 11967 (1990).